

# Long range proximity effect in $\text{La}_{2/3}\text{Ca}_{1/3}\text{MnO}_3$ / $(100)\text{YBa}_2\text{Cu}_3\text{O}_{7-\delta}$ ferromagnet/superconductor bilayers: Evidence for induced triplet superconductivity in the ferromagnet.

Yoav Kalcheim,<sup>1</sup> Tal Kirzhner,<sup>2</sup> Gad Koren,<sup>2</sup> and Oded Millo<sup>1</sup>

<sup>1</sup>*Racah Institute of Physics and the Hebrew University*

*Center for Nanoscience and Nanotechnology,*

*The Hebrew University of Jerusalem, Jerusalem 91904, Israel*

<sup>2</sup>*Department of Physics, Technion-Israel Institute of Technology, Haifa 32000, Israel*

## Abstract

Scanning tunneling spectroscopy measurements conducted on epitaxially grown bilayers of half-metallic ferromagnetic  $\text{La}_{2/3}\text{Ca}_{1/3}\text{MnO}_3$  (LCMO) on superconducting (SC)  $(100)\text{YBa}_2\text{Cu}_3\text{O}_{7-\delta}$  (YBCO) reveal long-range penetration of superconducting order into the LCMO. This anomalous proximity effect manifests itself in the tunneling spectra measured on the LCMO layer as gaps and zero bias conductance peaks. Remarkably, these proximity-induced spectral features were observed for bilayers with LCMO thickness of up to 30 nm, an order of magnitude larger than the expected ferromagnetic coherence length in LCMO. We argue that this long-range proximity effect can be accounted for by the formation of spin triplet pairing at the LCMO side of the bilayer due to magnetic inhomogeneity at the interface or at domain walls. Possible symmetries of the induced order parameter are discussed.

## Introduction

Significant research has been dedicated lately to the characterization of half metallic ferromagnets (HMF) motivated by their application in spintronics as sources of spin polarized current. The proximity effect in HMF – superconductor (SC) junctions has also drawn much attention recently due to its possible application in magnetization controlled Josephson junctions[1] and more generally, as means for investigating the interplay between the competing orders of ferromagnetism (F) and SC. The underlying mechanism of the proximity effect (PE) in a normal metal (N) in good electrical contact with a SC is the Andreev reflection (AR) whereby a hole-like quasiparticle from the N side impinging on the interface is retro-reflected as an electron-like quasiparticle with opposite spin, destroying a Cooper pair on the SC side. By this, superconductivity is reduced in the SC side of the interface and pairing correlations and thus a SC order parameter (OP) are induced in N. At a finite temperature,  $T$ , superconducting correlations will be observed in N up to a distance  $\xi_N = \sqrt{\hbar D/k_B T}$  from the N-SC interface, where  $D$  is the diffusion coefficient. Beyond this so called 'normal coherence length', typically of the order of ten of nm, the hole-like and electron-like quasiparticles start losing phase coherence. The AR process, or the PE, are naturally expected to be drastically suppressed at F-SC interfaces due to the exchange interaction in F. Indeed, by applying the methodology originally introduced by Fulde, Ferrel, Larkin and Ovchinnikov (FFLO)[2, 3] for treating magnetic superconductors to the problem of F-SC junctions, it was shown[4, 5] that the exchange field  $E_{ex}$  in F, reduces the coherence length in the ferromagnet,  $\xi_F$ , to  $\hbar v_F/2E_{ex}$  in the clean limit (where  $v_F$  is the Fermi velocity) and to  $\sqrt{\hbar D/2E_{ex}}$  in the dirty limit, both of which are typically of the order of 1 nm.

However, recent studies on NbTiN-CrO<sub>2</sub>-NbTiN (SC-HMF-SC)[1] and Nb-Cu<sub>2</sub>MnAl-Nb (SC-intermetallic F-SC) [6] Josephson junctions revealed a long range PE where the supercurrent between the two SC electrodes was measured even when the F-layer thickness was much larger than  $\xi_F$ . Keizer et al.[1] attributed their findings to the formation of a triplet pairing component at the CrO<sub>2</sub> – NbTiN interfaces, as predicted by Bergeret, Volkov and Efetov[7] and by Eschrig et al.[8]. The long range Josephson effect reported by Sprungmann[6] was similarly attributed by Linder and Sudbo[9] to triplet pairing, formed due to spin-active zones in the Nb-Cu<sub>2</sub>MnAl interfaces. A triplet component with parallel spins can support AR, in a similar manner as in singlet pairing in N-SC junctions, giving rise

to a PE on a length scale comparable to  $\xi_N$ . The orbital symmetry of the induced triplet pairing correlations may be either even (s-wave, d-wave) or odd (p-wave, f-wave), corresponding, respectively, to an odd or even dependence on the Matsubara frequency[10, 11].

Long range Josephson coupling was found also for junctions consisting of the high temperature superconductor  $\text{YBa}_2\text{Cu}_3\text{O}_{7-\delta}$  (YBCO) and the itinerant ferromagnet  $\text{SrRuO}_3$ (SRO) [12]. Subsequently, STM measurements [13] suggested that this long range proximity effect (LRPE) may take place only locally, along the domain walls (DWs) of the SRO. The tunneling  $dI/dV$  *vs.*  $V$  spectra revealed proximity superconducting gaps on the surface of SRO layers much thicker than the expected  $\xi_F$ , but these were confined to strips of width consistent with the DW size of SRO. Thus, they attributed the local LRPE to the crossed Andreev reflections (CARE) process[14, 15], whereby a hole impinging on the interface in one magnetic domain is retro-reflected as an electron with opposite spin polarization in an adjacent domain having opposite magnetization. It should be noted that this process can take place only if the DW width is up to a few times larger than coherence length in the SC side of the junction,  $\xi_S$ [16], which is  $\sim 2$  nm in YBCO. Volkov and Efetov[17], on the other hand, attributed this LRPE to the formation of an odd-frequency triplet s-wave pairing component in the DWs of F.

In order to check whether the CARE process is indeed essential for LRPE we studied in this work bilayers of YBCO coated by the HMF  $\text{La}_{2/3}\text{Ca}_{1/3}\text{MnO}_3$  (LCMO). The DW width in thin LCMO films at 4.2 K is estimated[18] to be  $\sim 20$  nm (although this value may depend on substrate, preparation process and film thickness), which is much larger than  $\xi_S$  in YBCO and thus the CARE process should be largely suppressed. Surprisingly, our tunneling spectra revealed spectroscopic features conforming to proximity-induced superconductivity even on LCMO layers as thick as 30 nm, an order of magnitude larger than the FFLO predicted  $\xi_F$ . Moreover, these features were not confined only to narrow strips (as in our previous study[13] of SRO/YBCO bilayers) and *both* gaps and zero bias conductance peaks (ZBCP) were measured. Our data suggest, as discussed below, that proximity-induced triplet-pairing in LCMO plays an important role in the PE observed in our samples. In a recent experiment, evidence for proximity induced triplet pairing at the SC side of F/SC (In/Co or In/Ni) junctions was provided [19]. In our present work, on the other hand, the proximity induced triplet correlations are found on the F side.

## Experimental

We have studied epitaxial bilayers consisting of LCMO films deposited on optimally doped  $a$ -axis (100)YBCO films grown by laser ablation deposition on (100)SrTiO<sub>3</sub> (STO) substrates. The YBCO was deposited on the STO wafer in two steps. First a 45 nm thick template layer of YBCO was deposited at a wafer temperature of 600 °C. Then a second 90 nm thick YBCO layer was prepared at 750 °C. The surface area of the YBCO consisted of 95% (100)YBCO (verified by x-ray diffraction) with no traces of (110) orientation found. The LCMO layers were grown on top of the YBCO at 790 °C and annealed for one hour at 450 °C in 0.5 Atm oxygen environment. The whole process was performed *in situ* without breaking the vacuum, and given the good lattice matching between YBCO and LCMO, high interface transparency could be obtained, important for the AR process to take place. The thickness of our LCMO layers ranged between 15 nm to 50 nm with surface roughness of  $\sim 1$  nm on top of the YBCO crystallites. Full coverage of the YBCO by LCMO was confirmed by x-ray photoelectron spectroscopy (XPS) and time of flight secondary ion mass spectrometry measurements. Magneto-resistance and resistance *vs.* temperature measurements of the samples reveal a ferromagnetic transition of the LCMO layer at  $\sim 250$  K and the SC transition of YBCO at  $\sim 88$  K, as presented in Fig. 1. It is important to note that  $a$ -axis YBCO films were chosen for this study, rather than the more common  $c$ -axis (001)YBCO films, since the PE is significantly suppressed along the  $c$ -axis[20, 21].

Samples were transferred in dry atmosphere to our cryogenic STM after being exposed to ambient air for less than 10 minutes. After evacuation the STM chamber was filled with He exchange gas at 1 Torr and then cooled down to 4.2 K where all the measurements presented here were performed, using a Pt-Ir tip. Several control measurements were performed at temperatures up to 150 K to verify that the spectroscopic features associated with SC (gaps and ZBCPs) indeed vanish above the  $T_c$  of YBCO. Topographic images were taken in the standard constant current mode with bias voltages  $\sim 100$  mV, well above the SC gap. The tunneling  $dI/dV$  *vs.*  $V$  spectra, which are proportional to the local density of states (DOS), were numerically derived from the I-V curves acquired on the LCMO surface while momentarily disconnecting the STM feed-back loop.

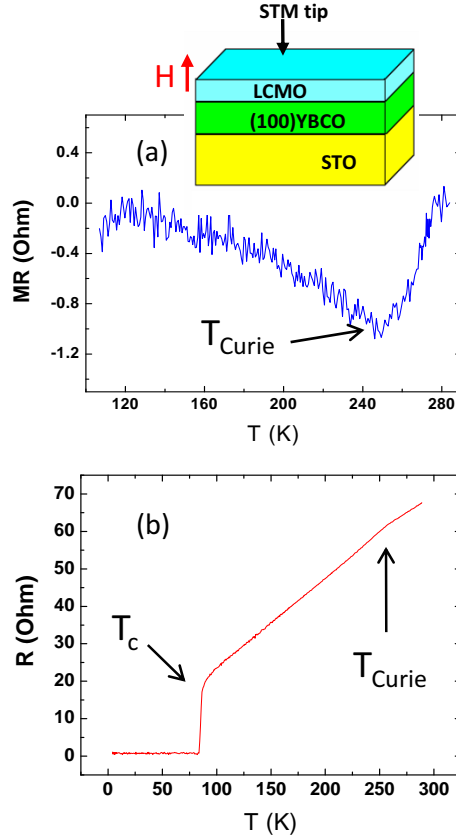


FIG. 1: (color online). (a) Magneto-resistance  $R(2T)-R(0)$  measurement of a 20 nm LCMO/(100)YBCO bilayer as a function of temperature showing the ferromagnetic transition at  $\sim 250$  K. The inset shows the structure of our samples, the direction of the magnetic field applied in the magneto-resistance measurement and the tunneling direction in the STM measurements (performed at  $H=0$ ). (b) Resistance vs. temperature curve of the same LCMO/YBCO bilayer depicting a superconducting transition at  $\sim 88$  K. The LCMO ferromagnetic transition is also manifested here, in the slope change at  $\sim 250$  K.

## Results

Tunneling  $dI/dV$  vs.  $V$  curves representing the most typical spectroscopic features found on our samples are portrayed in Fig. 2. Curves (a) and (b) do not show any SC-like features. Curve (a) exhibits a nearly constant metallic-like DOS while curve (b) exhibits a wide insulator-like gap structure. These spectra are very similar to those reported in Ref [22], corresponding to conductive and insulating regions, respectively, coexisting in LCMO

films. Regions exhibiting such features were found on all our samples, with abundance that grew with increasing LCMO thickness. However, in many regions smaller gaps, having suppressed SC coherence peaks (the so called ‘gap-like features’) at 8-10 mV were observed (c), indicative of PE due to the SC YBCO film. Interestingly, ZBCPs also appeared within such ‘gapped areas’, although less frequently. The ZBCP were found to be either embedded within a gap-like feature (curve (e)) or not (curve (f)), and in some cases showed splitting (see below). We recall here in passing that the ZBCP is one of the hallmarks of anisotropic sign-changing order parameters, such as  $p$ -wave or  $d$ -wave. The SC-like spectroscopic features were observed on large areas of the 15-20 nm thick LCMO samples, but their abundance decreased with LCMO thickness. No such features were detected for the 50 nm LCMO thickness bilayer, on which only the aforementioned metallic- and insulating-like spectra were measured. It is also important to note that SC-like features were not observed above the  $T_c$  of YBCO for all bilayers, indicating that they are indeed associated with the PE.

We shall now discuss the spatial distribution of regions where SC-like features appeared. On few occasions the gaps were confined to well-defined strips,  $\sim 40$  nm wide, bordered by regions exhibiting metallic-like spectra (Ohmic I-V curves), as shown in Fig. 3. The resemblance of the line width to that of the DW in LCMO suggests that in these cases the spectra were acquired over a DW where the PE may be locally enhanced, as found in Ref. [13]. We note that the locations of such lines showed no correlation with any specific topographic feature. However, most commonly gaps were not confined to such narrow lines and appeared to be spread over much larger areas, as demonstrated by Fig. 4. Typically, these regions were surrounded by areas characterized by the wide ‘insulating gap’ (such as curve (b) in Fig. 2), where the LCMO was presumably more insulating and thus less likely to allow PE. The spectra acquired along lines presented in Fig. 4 show that the proximity SC gaps varied spatially in both their width and zero bias conductance. However, on average, the gaps became shallower with increasing (nominal) LCMO layer thickness as depicted in Fig. 5. Since the gaps’ zero bias conductance varied spatially within each sample (see Figs. 3 and 4), we present in Fig. 5, for each LCMO thickness, an average spectrum calculated over regions of a few  $100\text{ nm}^2$  where gaps having the lowest zero bias conductance (deepest gaps) were observed.

In contrast to the previous report by Asulin et al. [13], where only proximity gaps were observed for the SRO/YBCO bilayers, in the present study also ZBCPs appeared within

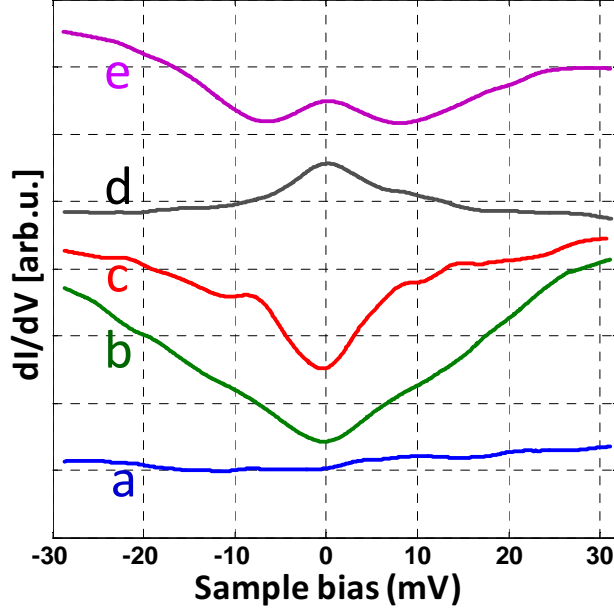


FIG. 2: (color online). Tunneling  $dI/dV$  vs.  $V$  spectra acquired at 4.2 K on LCMO/(100)YBCO bilayers showing the five main different spectral features measured on these F/SC bilayers (shifted for clarity). Curves (a) and (b) show no signature of a PE, where presumably, curve (a) was acquired over a metallic LCMO region and curve (b) was taken on a more insulating region. The upper three curves manifest proximity-induced SC order in the LCMO layer. Curve (c) shows the most prominent such spectral feature that appeared in our measurements, a SC-like gap in the DOS, whereas (d) and (e) portray ZBCPs, indicative of a sign-changing ( $p$ -wave or  $d$ -wave) order parameter. The ZBCPs and gaps appeared even on LCMO layers of 30 nm thickness (curve (d)) but not on 50 nm thickness and not above  $T_c$ , indicating a long-range proximity effect that we attribute to induced triplet pairing.

‘gapped regions’, as demonstrated by Fig. 4(d and f). No unique topographical feature that could be associated with the nodal (110)YBCO surface was found in those regions. The ZBCPs were significantly less abundant in our tunneling spectra compared to the gaps, and moreover, they were not always robust and sometimes disappeared upon repeating the I-V measurement at the same spot, turning into gaps. This may be due to the effect of the measurement itself, but nevertheless further indicates that the ZBCPs did not arise due to any YBCO faceting effect, and suggests that PE is the common origin of both ZBCPs and gaps in the DOS measured on the LCMO surface.

In some cases more complex spectra were measured, such as very small peaks within

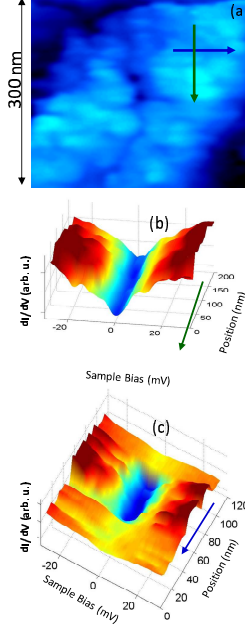


FIG. 3: (color online). STM measurement of the evolution of the local DOS ( $dI/dV$  vs.  $V$  tunneling spectra) along two transverse lines on a 15 nm LCMO/(100)YBCO bilayer. The gaps in the DOS along the green and blue lines are shown in (b) and (c) respectively. These data suggest that the LRPE in this region may be mediated by a domain wall. The width of the 'gapped' region in (c),  $\sim 40$  nm, is of the order of the domain wall width in LCMO, suggesting that in this case the LRPE is mediated by the presence of a domain wall.

gaps, as shown in Fig. 6(a) and split ZBCPs, with splitting of a few meV (Figs. 6(b) and 6(c)). Interestingly, the spectra presented in each panel of Fig. 6 were taken along a single line of length less than 300 nm, yet large variations from pure gaps or ZBCPs to the more complex structures are observed. As will be further discussed below, the complex spectra may indicate co-existence of two kinds of pairing symmetries, as predicted in Ref. [11].

## Discussion

Our measurements clearly show that LRPE is a robust phenomenon existing over large parts of LCMO/(100)YBCO bilayers. As discussed earlier, a mechanism based on the FFLO model cannot account for PE to distances larger than a few nm. In addition, the CARE-based LRPE scenario discussed in Refs. [13, 16, 23] is also inapplicable here since the length scale over which the magnetization direction can change, and in particular the DW width,

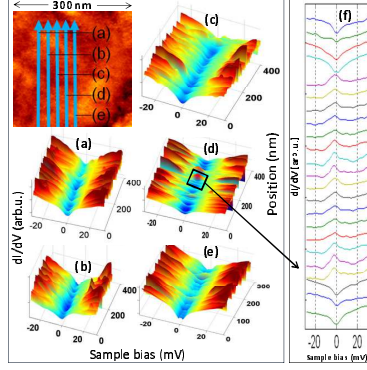


FIG. 4: (color online). STM measurements of the local DOS of a 17 nm LCMO/(100)YBCO bilayer showing SC-like features that are not confined to domain walls. [(a)-(e)] tunneling spectra taken along the indicated (representative) lines. Gaps in the DOS have been observed in areas of over 500nm x 100nm, far wider than LCMO's typical domain wall width of  $\sim 20$  nm. (f) Tunneling spectra (shifted for clarity) taken along the marked part of line (d) showing ZBCPs that appeared over a typical length scale of 10 nm.

is much larger than the coherence length in YBCO. We note in this regard that the CARE effect is predicted to be very small even when the DW width is  $5\xi_S$  ( $\sim 10$  nm in YBCO), quite narrower than the DW in LCMO. Therefore, induced triplet-pairing in LCMO appears to be the most probable mechanism by which PE is mediated in our samples.

An interesting question that arises now is the orbital symmetry of the induced triplet-pairing OP in the LCMO film. According to the Pauli principle, if the Cooper pair wave-function is symmetric in spin space, as in a triplet state, then it must be asymmetric in momentum space. Consequently, triplet-pairing SCs are assumed to have  $p$ -wave orbital symmetry. Such a dependence on momentum, however, makes superconductivity sensitive even to non-magnetic impurity (Anderson's theorem[24]) and should not survive in disordered systems. Indeed, superconductivity in ferromagnetic  $Sr_2RuO_4$ , where singlet pairing is prohibited due to the exchange field, was found to be of triplet  $p$ -wave pairing, and has been observed only in clean samples [25]. However, another mechanism for triplet pairing (originally proposed by Berezinsky [26] for superfluid  $^3He$ ) enables the pair wave-function to abide by Pauli's principle by being symmetric in momentum space and an odd function of the Matsubara frequency. A corresponding odd frequency spin-triplet  $s$ -wave pairing is thus not sensitive to impurity scattering and can therefore survive in F over a length scale

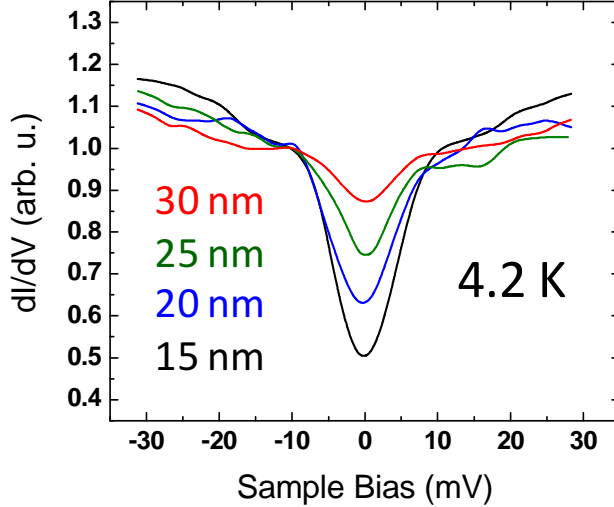


FIG. 5: (color online). Averaged tunneling spectra at 4.2 K measured on a LCMO/YBCO bilayer with varying LCMO thickness, as indicated. Each curve represents an average over spectra acquired at regions where the gaps were most pronounced, having the lowest zero bias conductance.

of the order  $\xi_N \gg \xi_F$ , like in ‘conventional’ N-SC proximity systems. Bergeret, Efetov and Volkov showed that such pairing can be promoted by magnetic inhomogeneity, either at the F/SC interface[7, 10] or at DWs [17], giving rise to LRPE. Eschrig et al. [8, 11] addressed the problem of LRPE in HMF-SC junctions. They model a spin active interface causing spin-mixing and breaking of the spin rotation symmetry. Such an interface is formed, for instance, if there is a misalignment of the magnetic moment at the F/SC interface with respect to that of the F bulk. In this scenario, OPs of even frequency  $p$ - or  $f$ -wave and odd frequency  $s$ - or  $d$ -wave symmetries are induced in the HMF with relative amplitudes that depend on the amount of disorder.

Proximity-induced odd-frequency triplet  $s$ -wave pairing in the LCMO side of our bilayers can well account for the gaps in the DOS we observed on large regions of our samples having LCMO thicknesses as large as 30 nm (see Fig. 5). According to Ref. [7] the SC correlations are expected to penetrate the F up to a distance over which the magnetization changes its orientation which is of the order of the DW width, ( $\sim 20$  nm in LCMO), consistent with our findings. This mechanism[17] may also apply to the measurements in which gaps appeared along lines conforming to the LCMO’s DW structure. The variations in the gap width and zero bias conductance along the surface, and in particular the presence of areas showing metallic-like and insulating-like DOS along with regions exhibiting clear proximity SC spec-

tral features may be due to spatial variations in the LCMO/YBCO interface transparency, LCMO film properties, and the possible presence of an underlying  $c$ -axis YBCO crystallite (where PE is suppressed).

Even more intriguing than the proximity induced gaps are the ZBCPs that were found, although less abundantly compared to the gaps, on all our bilayers with LCMO thickness up to 30 nm. Odd triplet  $s$ -wave OP cannot account by itself for the appearance of ZBCPs since an anisotropic OP that changes its sign at the Fermi surface is required for their formation (and the correction to the DOS at zero bias predicted in Ref.[17] is much smaller than our measured ZBCPs). The two most probable candidates for such an OP have either  $d$ -wave or  $p$ -wave symmetry, where ZBCPs are found for tunneling along the nodal or anti-nodal directions, respectively[27–29]. In the case of  $d$ -wave symmetry it was shown[30] that ZBCPs may also arise in  $c$ -axis tunneling due to impurity scattering. As discussed above, the ZBCPs that we measured on LCMO are most probably not associated with nodal (110) facets of the underlying  $d$ -wave YBCO SC. We thus attribute them to the penetration of either odd-frequency triplet  $d$ -wave or even-frequency triplet  $p$ -wave order into the LCMO film by either of the ZBCP-formation mechanisms discussed above. It is possible that the small and rather scarce regions where ZBCPs appeared contained less disorder than other parts of the sample and thus anisotropic pairing could survive. As mentioned earlier, the ZBCPs were rather fragile, and they sometimes disappeared after measurements at a specific location, turning into gaps. This suggests that ZBCPs are indeed related to an unstable OP that may be affected by the possible influence of the STM measurement on local disorder. It should be noted here that although the current typically applied in STM measurements is quite low, reaching about 0.1 nA in our case, the corresponding current densities are rather high and therefore STM measurements can become quite perturbative. Unfortunately, our spectra do not allow us to state whether the ZBCPs are due to induced  $d$ -wave or  $p$ -wave pairing, since there are many parameters that one can play with in fitting the data to the extended BTK models for tunneling into  $d$ -wave[27] or  $p$ -wave[28, 29] OP symmetries. Nevertheless, in some cases the rather large width of the ZBCP conforms better to  $p$ -wave pairing (such as the black curve in Fig. 2).

In addition to spectral features showing pure gaps or ZBCPs, indicative of a single component OP, we have also measured more complex spectral structures, such as peaks embedded within gaps or split ZBCPs, as demonstrated by Fig. 6. Remarkably, the transition from the

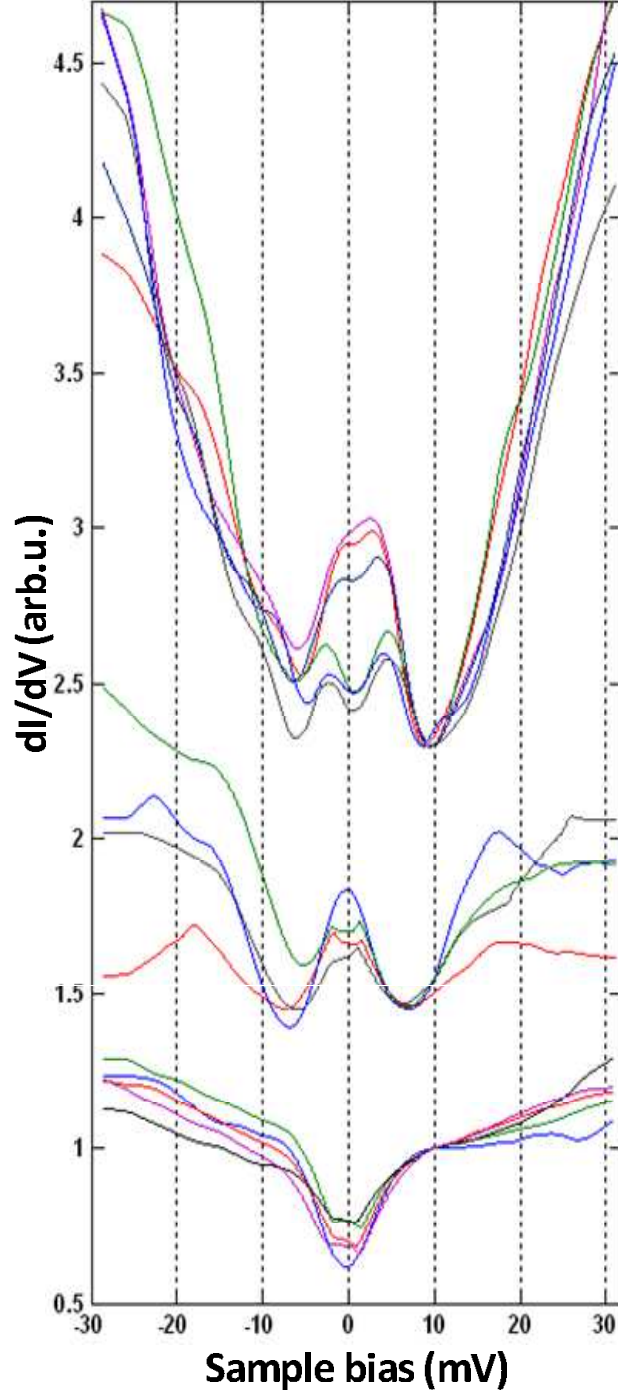


FIG. 6: (color online). Tunneling spectra acquired along lines of length smaller than 100 nm on 17 nm LCMO/YBCO bilayer (a) and 20 nm LCMO/YBCO bilayer [(b) and (c) - (shifted for clarity after normalization to the dip at positive voltage)], showing transitions from pure gap structure to a small peak within a gap (a) and evolution of ZBCP splitting [(b) and (c)]. These data may be attributed to mixed induced-OP symmetries (*s*- *p*- and *d*-wave) with relative amplitudes varying along the sample.

'simple' to 'complex' structures, as well as significant spatial evolution of the latter, namely, development of the embedded peak or ZBCP splitting, took place over distances of the order of 10-100 nm. The emergence of the ZBCP within the gap, shown in Fig. 6(a), may be due to changing the tunneling direction with respect to the main symmetry axes of the ( $d$ -wave or  $p$ -wave) OP. This, however, cannot account for the ZBCP splitting. More likely, the spectra presented in Fig. 6 may reflect the formation of a complex OP, namely, contributions with spatially varying degrees of relative magnitude of  $s$ -,  $p$ - and  $d$ -wave components, possibly with phase shifts between them that may yield ZBCP splitting[31–34]. We note in passing that spatial variations of the sub-dominant component ( $s$  or  $d_{xy}$ ) of the complex OP  $d+is$  or  $d+id_{xy}$ , was recently observed by Ngai et al. on (110) $\text{Y}_{0.95}\text{Ca}_{0.05}\text{Ba}_2\text{Cu}_3\text{O}_{7-\delta}$ [35]. Alternatively, there have also been theoretical suggestions that the spontaneous peak splitting can arise extrinsically, from either electron-hole asymmetry, multiband effects or magnetic impurity perturbation [36–38]. Further studies are needed to resolve these issues.

## Summary

In this paper we have used scanning tunneling spectroscopy to investigate the local density of states on the LCMO surface of LCMO/(100)YBCO (HMF/SC) bilayers. We found clear evidence for long range proximity effect manifested as gaps and ZBCPs in the tunneling spectra. These effects survived for LCMO film thicknesses of up to  $\sim 30$  nm, an order of magnitude larger than the coherence length  $\xi_F$  in LCMO expected from the standard FFLO theory. Unlike the case of a previous study on SRO/YBCO bilayers[13], the CARE mechanism cannot account for the LRPE due to the large width of DWs in LCMO. Triplet pairing in the HMF LCMO is suggested to be the underlying mechanism for the observed LRPE. Gaps in the DOS abundant over very large portions of our samples can be accounted for by odd frequency triplet  $s$ -wave pairing, which can survive over long distances due to its insensitivity to impurity. The surprising appearance of ZBCPs along with more complex SC-like features in some regions suggest that the induced OP in LCMO has also  $p$ -wave or  $d$ -wave components along with the  $s$ -wave OP, with relative magnitude determined by the local impurity concentration.

## Acknowledgements

This research was supported in parts by the joint German-Israeli DIP Project, the United States—Israel Binational Science Foundation Grant No. 200808, the Harry de Jur Chair in Applied Science, and the Karl Stoll Chair in advanced materials.

---

- [1] R. S. Keizer, S. T. B. Goennenwein, T. M. Klapwijk, G. Miao, G. Xiao, and A. Gupta, *Nature* **439**, 825 (2006).
- [2] P. Fulde and F. A., *Phys. Rev.* **135**, A551 (1964).
- [3] A. Larkin and O. Y., *Sov. Phys. JETP* **20**, 762 (1965).
- [4] E. Demler, G. Arnold, and M. Beasley, *Phys. Rev. B* **55**, 15174 (1997).
- [5] A. I. Buzdin, *Rev. Mod. Phys.* **77**, 935 (2005).
- [6] D. Sprungmann, K. Westerholt, H. Zabel, M. Weides, and H. Kohlstedt, *Phys. Rev. B* **82** (2010).
- [7] F. S. Bergeret, A. F. Volkov, and K. B. Efetov, *Phys. Rev. Lett.* **86**, 4096 (2001).
- [8] M. Eschrig, J. Kopu, J. C. Cuevas, and G. Schön, *Phys. Rev. Lett.* **90**, 137003 (2003).
- [9] J. Linder and A. Sudbo, *Phys. Rev. B* **82** (2010).
- [10] F. S. Bergeret, A. F. Volkov, and K. B. Efetov, *Rev. Mod. Phys.* **77**, 1321 (2005).
- [11] M. Eschrig and T. Loefwander, *Nat. Phys.* **4**, 138 (2008).
- [12] L. Antognazza et. al., *Appl. Phys. Lett.* **63**, 1005 (1993).
- [13] I. Asulin, O. Yuli, G. Koren, and O. Millo, *Phys. Rev. B* **74**, 092501 (2006).
- [14] J. Byers and M. Flatte, *Phys. Rev. Lett.* **74**, 306 (1995).
- [15] G. Deutscher and D. Feinberg, *Appl. Phys. Lett.* **76**, 487 (2000).
- [16] W. J. Herrera, A. L. Yeyati, and A. Martin-Rodero, *Phys. Rev. B* **79**, 014520 (2009).
- [17] A. F. Volkov and K. B. Efetov, *Phys. Rev. Lett.* **102** (2009).
- [18] M. Ziese, S. P. Sena, and H. J. Blythe, *J. Magn. Magn. Mater.* **202**, 292 (2001).
- [19] B. Almog, S. Hacohe-Gourgy, A. Tsukernik, and G. Deutscher, *Phys. Rev. B* **80**, 220512(R) (2009).
- [20] H. Z. Durusoy, D. Lew, L. Lombardo, A. Kapitulnik, T. H. Geballe, and M. R. Beasley, *Physica C* **266**, 253 (1996).

- [21] A. Sharoni, I. Asulin, G. Koren, and O. Millo, Phys. Rev. Lett. **92**, 539 (2004).
- [22] S. Chen, P. Lin, J. Juang, T. Uen, K. Wu, Y. Gou, and J. Lin, Appl. Phys. Lett. **82**, 1242 (2003).
- [23] P. Aronov and G. Koren, Phys. Rev. B **72**, 184515 (2005).
- [24] J. R. Schrieffer, *Theory of Superconductivity* (W. A. Benjamin, Inc., New York, 1964).
- [25] G. Luke, Y. Fudamoto, K. Kojima, M. Larkin, J. Merrin, B. Nachumi, Y. Uemura, Y. Maeno, Z. Mao, Y. Mori, H. Nakamura, and M. Sigrist, NATURE **394**, 558 (1998).
- [26] V. L. Berezinskii, JETP Lett. **20**, 287 (1974).
- [27] S. Kashiwaya, Y. Tanaka, M. Koyanagi, H. Takashima, and K. Kajimura, J. PHYS. CHEM. SOLIDS **56**, 1721 (1995).
- [28] M. Yamashiro, Y. Tanaka, Y. Tanuma, and S. Kashiwaya, PHYSICA C **293**, 239 (1997).
- [29] L. Xiao-Wei, Commun. Theor. Phys. **44**, 381 (2005).
- [30] S. H. Pan, E. W. Hudson, K. M. Lang, H. Eisaki, S. Uchida, and J. C. Davis, Nature **403**, 746 (2000).
- [31] M. Fogelstrom, D. Rainer, and J. Sauls, Phys. Rev. Lett. **79**, 281 (1997).
- [32] R. Laughlin, Phys. Rev. Lett. **80**, 5188 (1998).
- [33] C. Tsuei and J. Kirtley, Rev. Mod. Phys. **72**, 969 (2000).
- [34] G. Annunziata, M. Cuoco, C. Noce, A. Sudbo, and J. Linder, arXiv:1009.3014 (2010).
- [35] J. H. Ngai, R. Beck, G. Leibovitch, G. Deutscher, and J. Y. T. Wei, Phys. Rev. B **82**, 054505 (2010).
- [36] A. Golubov and F. Tafuri, Phys. Rev. B **62**, 15200 (2000).
- [37] Y. Tanuma, K. Kuroki, Y. Tanaka, and S. Kashiwaya, Phys. Rev. B **68** (2003).
- [38] Y. Asano, Y. Tanaka, and S. Kashiwaya, Phys. Rev. B **69**, 214509 (2004).